A novel hybrid MPPT technique for solar PV applications using perturb & observe and fractional

A novel hybrid MPPT technique for solar PV applications using perturb & observe and fractional open circuit voltage techniques

Ali F Murtaza[1], Hadeed Ahmed Sher[2], Chiaberge M[3], Boero D[1], De Giuseppe M[1] and Khaled E Addoweesh[2]
[1] Department of Mechanical and Aerospace Engineering,Politecnico di Torino,Turin, Italy
[2]Department of Electrical Engineering, King Saud University, Riyadh
[3]Department of Electronics and Telecommunication Engineering, Politecnico di Torino, Turin, Italy
Corresponding E-mail: ali.murtaza@polito.it

***Abstract*—Solar photovoltaic (PV) systems have been an area of active research for the last few decades to improve the efficiency of solar PV module. The non-linear nature of IV curve of solar PV module demands some technique to track the maximum voltage and maximum current point on IV curve corresponding to Maximum Power Point(MPP). Thus, Maximum Power Point Tracking (MPPT) techniques are widely deployed for this purpose. Lot of MPPT techniques have been developed in recent past but still most commercial systems utilizes the perturb & observe $(P\&O)$ MPPT technique because of its simple algorithm, low cost and ease of implementation. However, this technique is slow in tracking MPP under rapidly changing irradiance conditions and it also oscillates around the MPP. This paper addresses this problematic behavior of $P\&O$ technique and hence presents a novel MPPT hybrid technique that is combination of two basic techniques i.e. $P\&O$ and Fractional Open Circuit Voltage (FOCV) technique in order to overcome the inherited deficiencies found in $P\&O$ technique. The proposed MPPT technique is much more robust in tracking the MPP even under the frequent changing irradiance conditions and is less oscillatory around the MPP as compared to $P\&O$. The technique is verified using MATLAB/SIMULNK and simulation results show a clear improvement in achieving the MPP when subjected to change in irradiance.**

***Index Terms*—Solar PV, Modeling & Simulation, Hybrid MPPT, Perturb & Observe, Fractional open circuit voltage**

I. Introduction

In the recent decade the use of alternate energy sources for power generation has gained a lot of importance due to their eco friendly nature and abundance of availability without any cost. However, solar photovoltaic has gained tremendous importance due to technological advancements in achieving energy efficiency and reduced cost. The solar PV systems (arrays) however, can not deliver the maximum power automatically and it showed non-linear dynamic behavior, thus it has non liner I-V curve. The traditional work in this regard is mostly related in tracking the point on I-V curve which ensures maximum power at the output. Therefore, MPPT technique to track MPP on I-V curve becomes of great importance. The duty of MPPT therefore is to get maximum efficiency and to operate the system around MPP. The variety of available MPPT techniques in literature are summarized by T.Ersam in a form of a survey and he concluded that out of 19 distinct methods found in literature following three methods are most widely used [1].

- Perturb and Observe $(P\&O)$
- Incremental conductance
- Fractional Open Circuit Voltage method (FOCV)

These days, most of the research in MPPT is directed towards the improvement of three basic MPPT methods by inducting the intelligent mechanism like artificial intelligence, neural networks, fuzzy logic and complex control techniques. Few hybrid techniques are also available in the literature for tracking MPPT. [2], [3]. One research paper introduces the waiting function in $P\&O$ and consider the fact that if algebraic sign of the perturbation is reversed several times in a row, it means that MPP has been reached [4]. This idea works well under constant irradiance but will struggle more under rapid irradiance as it needs more time to track the MPP of new irradiance. Another idea is of inducting the three-point weight comparison in $P\&O$ has been proposed by [5]. It will perturb from one point to another and then doubly perturb in the opposite direction to reach another point, and then by comparison of these three points, a decision is made about the next perturbation sign. It gives the idea of irradiance changing. But again, moving forward and backward increases the number of samples and slows the speed of the algorithm. In [6] two stage algorithm is proposed in which it exhibits faster tracking in the first stage while fine tracking in the second stage. This work is modified by [7] as it bypasses the first stage using nonlinear equation to measure the point close to MPP. But, the decision to switch from one stage to another or skipping the first stage is not very robust and also during fine tracking if irradiance gets changed then algorithm may be in trouble. The optimized $P\&O$ is proposed in [8] but is linked with the hardware topology used.

Keeping in view the above mentioned problems we present here novel algorithm / technique to compute the MPP. Our technique is a hybrid of $P\&O$ and fractional open circuit voltage and it is device intelligently in such a way that it adopts the advantages of the two techniques while rejecting their drawbacks. Mainly, we compare our results with $P\&O$

technique as it offers better results than fractional open circuit voltage. The proposed technique is designed to rectify two main issues of $P\&O$ i.e. it struggles to attain MPP under varying solar irradiance while oscillates around MPP under constant irradiance. The simulated results have shown clear improvement in attaining the MPP under rapidly changing environmental conditions. The time required to compute the MPP is also drastically reduced under dynamic environmental conditions, however it is same as of $P\&O$ under constant irradiance condition. Our mechanism is very different from [2] and is novel in nature. Furthermore, to reduce the cost of the system, temperature sensors are not incorporated in our design.

II. Modeling of Solar Array

Ideal solar PV cell is modeled as a current source with diode in parallel as shown in the fig.1. The equation that creates the I-V characteristics if the ideal PV cell [9]

$$I = I_{pv,cell} - I_{o,cell} exp((\frac{V_d}{nV_t}) - 1) \tag{1}$$

Where,

- $I_{pv,cell}$ is the current generated by incident light
- I_d is the Schokley diode current and is equal to $I_{o,cell} exp((\frac{V_d}{nV_t}) - 1)$
- $I_{o,cell}$ is leakage current
- V_d is the voltage across diode
- V_t is the thermal voltage of diode and is equal to $\frac{kT}{q}$
- q is the charge on electron
- k is Boltzmann constant
- $T$is temperature of $p-n$ junction,in Kelvin

Figure 1 shows the equivalent circuit of an ideal and practical PV cell. But, individual PV cell produces less power therefore, several cells are connected together in form of series-parallel combination to fabricate a PV module that has high output power at desired voltages [10]. Many practical PV modules are modeled in recent past but we have considered the single diode based practical model for PV modules as shown in fig.1. This model has a balance compromise between accuracy and simplicity [11]. Figure 2 shows the I-V and fig.3 shows the P-V curve of this model. In this model two practical resistances R_p & R_s has been added into ideal cell where, R_p represents the leakage current to the ground at the borders and R_s takes account for the internal losses due to current flow of the module. Therefore, eq.1 becomes,

$$I = I_{pv} - I_o exp((\frac{V + IR_s}{nV_t}) - 1) - \frac{V + IR_s}{R_p} \tag{2}$$

Where,

- I_{pv} and I_o are the PV and saturation currents of module respectively
- $V_t = N_s \frac{KT}{q}$ is the thermal voltage of the array with N_s cells connected in series

Kyocera KC200GT module is utilized to model the PV module according to eq.2 [9] and its parameters are shown in table I. However, the most difficult problem in the eq.2 is to

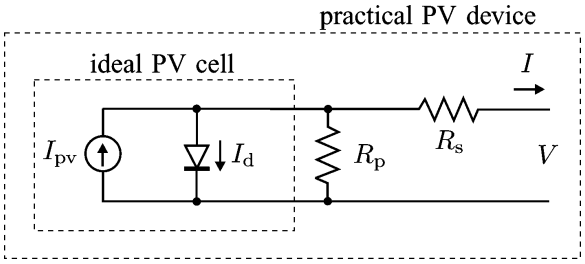

Fig. 1. Ideal PV cell and equivalent circuit of practical PV [12]

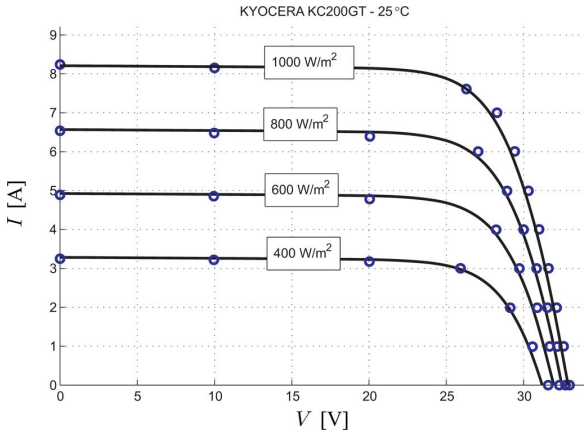

Fig. 2. I-V curve of solar PV cell used [9]

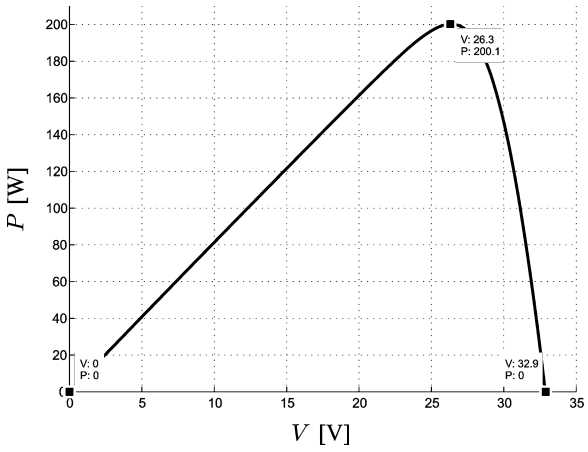

Fig. 3. P-V curve of PV cell [9]

measure R_s and R_p. This is because the relationships for these resistance are not available. Furthermore, manufacturer also hide such information in their data sheet. Therefore, assumptions are necessary. Normally, in practical module, the value of R_s is lower while value of R_p is high and by ignoring the small diode current, we can assume short circuit current $I_{sc} = I_{pv}$. This I_{pv} is linearly linked with solar irradiance and temperature as expressed by the eq.3

$$I_{pv} = (I_{pv,n} + K_I \Delta T) \frac{G}{G_n} \tag{3}$$

Where,

TABLE I
DATA SHEET OF KYOCERA KC200GT MODULE [12]

I_{mp}	7.61 A
V_{mp}	26.3 V
p_{max}	200.143 W
I_{sc}	8.21 A
V_{oc}	32.9 V
K_v	-0.1230 V/K
K_i	0.0032 A/K
N_s	54

- $I_{pv,n}$ is PV current at nominal condition
- K_I thermal co-efficient of current
- ΔT is change in temperature and in kelvin
- G is the irradiance on device surface
- G_n is the nominal irradiance

From table I, the $I_{pv,n}$ = $I_{sc,n}$=8.21 A and K_I=0.0032 A/K.

Consider the normal open circuit condition with V = $V_{oc,n}$, I=0 and $I_{pv} = I_{pv,n} = I_{sc,n}$, the diode saturation current I_o of the module with its dependence on the temperature can be calculated more accurately by inducting the thermal coefficients of current (K_I) and voltage (K_V) in eq.2 as follow [12]

$$I_{pv} = \frac{(I_{pv,n} + K_I \Delta T)}{(exp\frac{V_{oc,n}+K_v \Delta T}{nV-T}) - 1} \quad (4)$$

The values of R_s and R_p are only unknown from eq.2 are modeled from the fact that there is only one pair of R_s,R_p at which $P_{max,m} = P_{max,e} = V_{mp}I_{mp}$ at the V_{mp} , I_{mp} point of the I-V Curve [12]. Where, $P_{max,m}$ is the maximum power calculate by the I-V model of eq.2 and $P_{max,e}$ is the maximum experimental power from the data sheet. The values of R_s and R_p are further calculated by [12] and by using the table I the values of R_s and R_p are 0.221 and 415.405 ohms respectively. Finally, the model of PV array consists of fifteen serial and two parallel PV modules i.e. N_s = 15 & N_p = 2 is modeled in Matlab/SIMULINK and resulting graphs are illustrated in 4. This modeling is further used for verification of our MPPT algorithm.

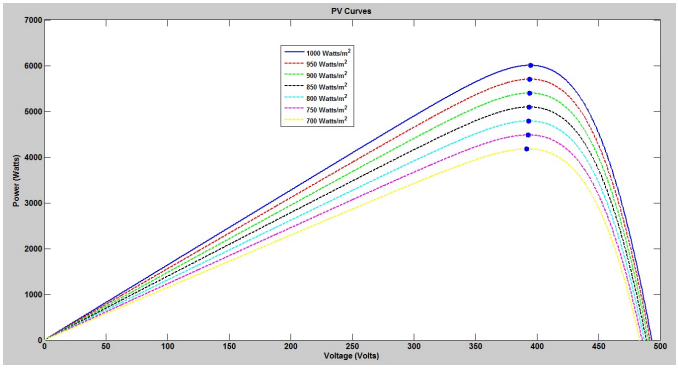

Fig. 4. PV curves of the modeled array

III. PROPOSED TECHNIQUE

Proposed technique is designed with more emphasis is put on $P\&O$ while taking help from FOCV method during confusing and critical situations. FOCV should only be used when very much necessary as measuring open circuit voltage leads towards the temporarily power loss. However, this method provides a very useful information about MPP which falls within the range of $0.7V_{oc}$ to $0.81V_{oc}$. With shift in irradiance and temperature values, V_{oc} also changes accordingly. Proposed technique is maintained in such a way that it gathers advantages of both $P\&O$ and FOCV while discarding their disadvantages. The proposed algorithm works in following three modes:

1) Mode 1: For region 1
2) Mode 2: For region 2 (Under changing irradiance)
3) Mode 3: For region 2 (Constant irradiance)

Each mode is specialized to deal with its specific scenario. Mode 1 is mainly involved to skip some area. Mode 2 is specialized to deal with changing environmental conditions with small step size as compared to step size used in $P\&O$. Mode 3 is designed to deal with steady state environmental condition with super small step size. Proposed technique mainly revolves around mode 2 and mode 3 with mode 2 ensures that power hovers around close to MPP even under irradiance and temperature changing conditions while mode 3 ensures that power oscillates significantly less around MPP under steady state environmental conditions. Flowchart of the algorithm is shown in fig.5.

1) Mode 1: Figure 6 shows a PV curve that is being divided into two regions. If region 1 is monitored closely, it can be noticed that whatever the environmental conditions and power is in region 1, backward movement should be avoided and always forward movement should be utilized so that region 2 can be reached as early as possible. Under any circumstances, MPP is normally present in region 2. It is further better if region 1 is completely skipped. Proposed technique utilizes the same idea in mode 1 that is to skip region 1 so that region 2 can be reached directly. But the problem here is to decide that where is the end of region 1 and start of region 2. For this purpose, the defacto principle has been used that the MPP for any environmental conditions is normally present in the region after $0.7V_{oc}$. Therefore proposed technique considers the region after $0.7V_{oc}$ as region 2. Mode 1 can be understandable by considering fig.7 and mode1 section in flowchart as shown in fig.5. Consider power curve P2 in fig.7. Proposed technique measures V_{oc} of P2 and then sets the operating voltage V_{op} at $0.7V_{oc}$ as shown in the flowchart. Power at that point is then measured and the technique proceeds in mode 2 as region 2 is started. In this way, regions 1 is being skip through a robust method by adjusting the operating voltage at $0.7V_{oc}$.

2) Mode 2: In mode 2, region 2 is reached and as MPP is not so far so small step sizes +/-ΔV_S are used. Small step size means that it has smaller step size as compared to step size utilized in traditional $P\&O$. To understand mode 2, consider mode 2 section in flowchart fig.5. In mode 2, first C- & C+ limits are cleared by the proposed technique and then current values of operating voltage $V_{op,c}$ and power $P_{op,c}$ are being stored. Then operating voltage V_{op} is being set at $0.76V_{oc}$ as MPP lies in region $0.7V_{oc}$ to $0.81V_{oc}$. An average is

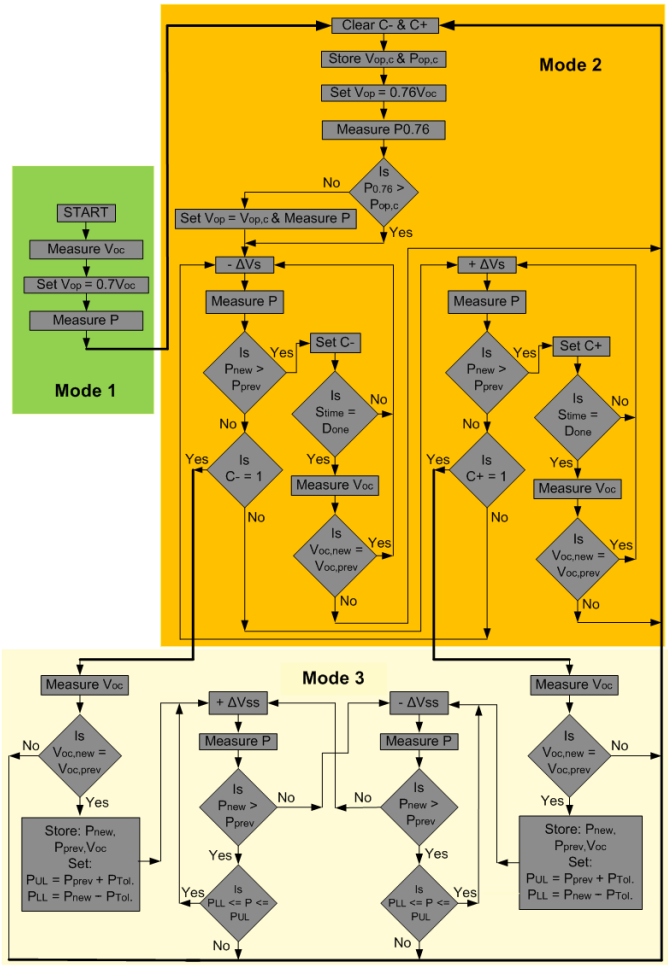

Fig. 5. Proposed Algorithm

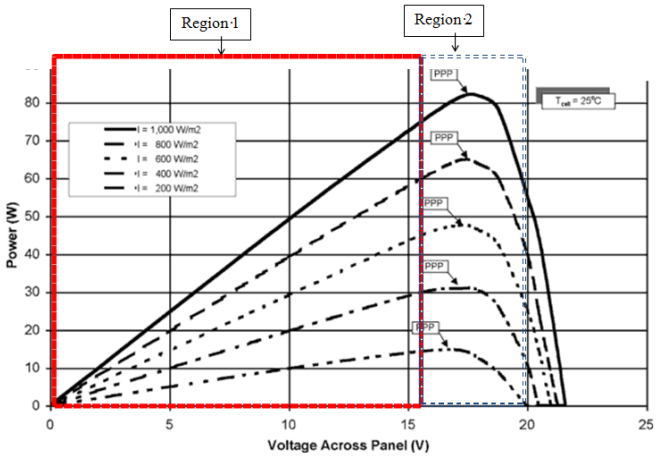

Fig. 6. Regional segregation of PV curve

considered, however any good value between 0.7 and 0.81 can be selected depending upon the type of photovoltaic modules. Power P0.76 is measured at an operating voltage equal to $0.76V_{oc}$ and then comparison is being made with last time power $P_{op,c}$. This comparison is utilized that may be $P_{op,c}$ is

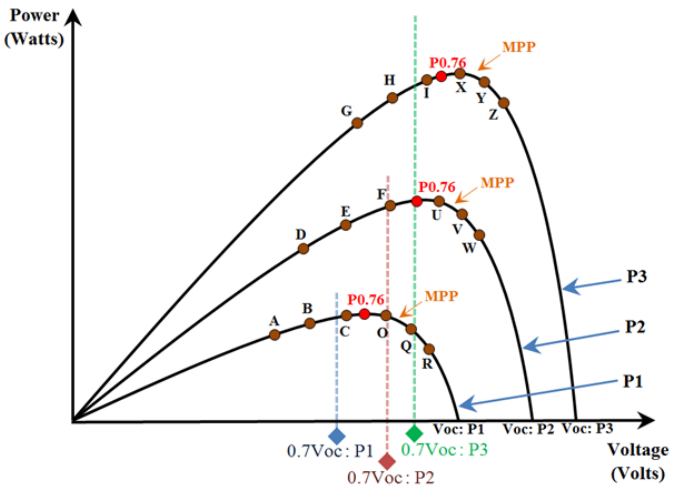

Fig. 7. PV curves with MPP under varying environmental conditions

already in a region closer to MPP as compared to P0.76, if this is the case then previous power $P_{op,c}$ will proceed otherwise P0.76 power. Consider fig.7 and say, point F is reached when we enter in mode 2. Clearly, power at point F is smaller than P0.76, so V_{op} with $0.76V_{oc}$ and P0.76 continue. Then V_{op} is perturbed with small negative step $-\Delta V_s$ and power condition is being checked. As P_{new} becomes smaller than P_{prev} so condition that C- is equal to 1 or not is being checked, which indicates that whether the area in which MPP lies, is reached or not. Which is clearly not as C- is not equal to 1. Proposed technique moves onto produce positive perturb in voltage i.e. $+\Delta V_s$. By taking ΔV_s, say point U at power curve P2 is reached. As P_{new} is greater than P_{rev} so C+ is set and then S_{time} is being checked. S_{time} is used here to measure V_{oc} after periodic intervals. V_{oc} is not measured in every step as it means a loss of power so it is checked periodically but its S_{time} should be optimized as such that no huge information is missed. Say S_{time} is not done so proposed technique moves back in loop to take another $+\Delta V_s$ and as a result point V is reached. It is clear from fig.7 that MPP of power curve P2 is present between points U & V. As P_{new} of point V becomes smaller than P_{prev} of U, so power condition breaks the loop and technique proceeds to check the C+ limit conditions. As C+ is already set last time, it means that area has been reached in which maximum power lies. So, the proposed technique moves onto mode 3 and working of mode 3 discussed afterwards. Consider the case that at point Q of P1, negative perturb in voltage is on. Suppose during $-\Delta V_s$, irradiance gets increased so point F of power curve P2 is reached instead of point O of power curve P1. As P_{new} of F is greater than P_{prev} of Q so C- is set as shown in the flowchart. Then S_{time} condition is checked as it is properly optimized so consider S_{time} is done. V_{oc} is measured by the proposed technique as new V_{oc} is not equal to previous V_{oc} so the loop is broken and proposed technique moves back to the starting point of mode 2. First limits C- & C+ are cleared and next storage of $V_{op,c}$ and $P_{op,c}$ of point F is done. Then V_{op}

is set at 0.76V_{oc} and power P0.76 is measured. By making comparison of P0.76 and $P_{op,c}$ of point F of power curve P2 it is clear that P0.76 is greater so V_{op} equal to 0.76 and power P0.76 continue. Proposed technique again move to -ΔVs for next cycle and say again irradiance gets changed and point H of curve P3 is reached. As P_{new} of H is greater than P_{prev} so C- will be set and sampling time condition is being checked again. Say S_{time} is done then again new V_{oc} is measured and is being compared with previous V_{oc}. As two V_{oc}'s are different so the proposed technique again moves back to mode 2. Cycle has been repeated again and V_{op} is again forced to operate at V0.76 as power of P0.76 is greater than $P_{op,c}$ of H. Therefore, whenever their is a change of irradiance, proposed technique always forces the V_{op} to remain close to that window in which maximum power is present unlike $P\&O$ which is continuously moving away from MPP. This process is only possible because of an innovative comparison with respect to P0.76. If value between 0.70 to 0.81 is chosen with proper calculations then the efficiency of power can be improved further. Although for the model that we are using, sound value is 0.81 but 0.76 value has been still utilized here just to prove the robustness of the proposed technique. Another thing if power is let us say far away from 0.76V_{oc} even then proposed technique works well as during comparison, V_{op} is not set at 0.76V_{oc} if the power is greater than P0.76.

3) Mode 3: Mode 3 is simple $P\&O$ mode with very small step sizes and additional power limits. It is pertinent to mention here that no one proposed power limits in the literature. To develop understanding about mode 3, consider mode 3 section in flow chat as shown in fig.5. As mode 3 is a steady state condition mode, so in start V_{oc} is measured first to confirm that during transition from mode 2 to mode 3 no irradiance or temperature gets changed. This is done by checking condition that whether V_{oc}, new is equal to V_{oc}, P_{prev} or not. Once, it is confirmed that the two V_{oc}'s are equal, then two limits lower power limit (PLL) & upper power limit (PUL) are being set with the involvement of power tolerances. Consider power curve P2 in fig.7. During mode 2 operation, P_{prev} is at U and P_{new} is at V when we entered in mode 3. Mode 3 in its operation, first measures V_{oc} and comparison is being made between $V_{oc,new}$ &$V_{oc,prev}$ to check that steady state condition of environment is still hanging. If it is true then V_{oc}, PUL and PLL are being stored. PUL & PLL values are calculated by the following equations:

$$PUL = P_{prev} + PowerTolerance \tag{5}$$

$$PLL = P_{new} - PowerTolerance \tag{6}$$

Power tolerances are included to be just on the safer side. Last time, P_{prev} is at point U while P_{new} is at point V and MPP is present in between them as shown in fig.8. With tolerance included, two limits PUL and PLL are calculated from equations A & B respectively and these limits represent points U‘ & V‘ as shown in fig.9. As in mode 3, step size has been so drastically reduced therefore MPP is trying to reach with +/-ΔV_{SS} by following red line and points shown

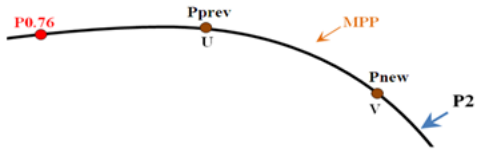

Fig. 8. Power curve P2 with detected MPP

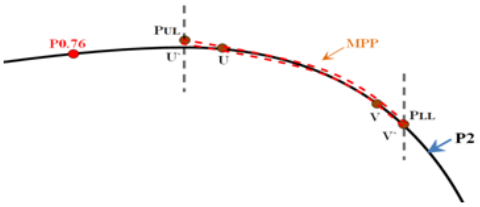

Fig. 9. Power curve P2 with limits PUL and PLL

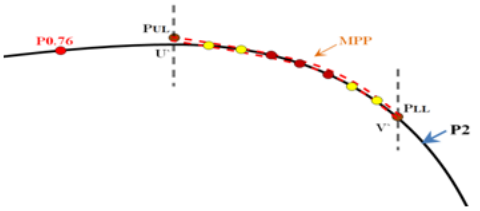

Fig. 10. Power curve P2 with step sizes points within limits

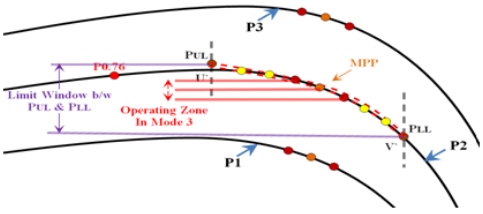

Fig. 11. Operation zone of different power curves

in fig.10. During this operation, once MPP is reached then the proposed technique has been significantly close hovering around MPP as shown by three brown points in fig.10. With super small step size (+/-ΔV_{SS}), proposed technique oscillate very less around MPP. During this no V_{oc} is measured then how technique gets the information that whether irradiance or temperature changes or not. This illustration is shown in fig.11. It can be seen from fig.11 that the limit window is occurred between PUL & PLL while proposed technique is operating in operating zone around MPP. Once, environmental condition changes, the effect would be produced like power curve P3 or power curve P1. In both cases, three points are shown on power curve P1 and power curve P3. As step sizes are very small and operating voltages are constant around MPP so if power curve P1 or P3 occurs during varying environmental conditions, then the new three points are shown on both power curves. In both case, three points either from P1 and P3 are out of limit window of PUL & PLL. Therefore, mode 3 flowchart can be seen from fig.5, it is understandable that every time

during positive or negative ΔVSS, limits are checked. As soon as limits are crossed, it means either irradiance or temperature is changed so the proposed technique moves back to mode 2 to settle down this issue. One thing should be noted here that as step size is super small and is moving around MPP in a very closed window that even a small change in irradiance will break the mode 3 which is what is required. So, in mode 3 an innovative work has been proposed by inducting the limits which has not been introduced previously in literature. With limits, measuring V_{oc} and therefore temporarily power loss has been avoided. Thus, proposed technique in mode 3 with its power limits and ultra small step size produces high efficiency of power and always hovering very close to MPP with almost negligible oscillations.

IV. Results and Discussion

The modeling and simulation of the proposed hybrid and traditional $P\&O$ techniques are performed in MATLAB environment and graphs are obtained. Graphs indicates the results in the form of power versus time of two techniques under constant and varying environmental conditions. Simulations are based on following sampling data and step sizes: for $P\&O$, large perturb in voltage i.e. ΔV_L = 7.4025 is being utilized while for proposed technique, small perturb in voltage ΔV_S = 3.4545 in mode 2 and super small perturb in voltage ΔV_{SS} = 1V is being utilized. Both techniques have the sampling rate of 15 msec. Two sections has been made, one showing the proposed technique versus conventional $P\&O$ under steady state conditions i.e. constant irradiance and constant temperature and the other one showing comparison of the two under dynamic conditions i.e. variations in both irradiance and temperature.

A. Steady State Conditions

Figure 12 shows the comparison between proposed technique and $P\&O$ under constant irradiance of 700 W/m^2 at 25 C°. Both techniques capture MPP well but it can be seen that proposed technique oscillates significantly less as compared to $P\&0$. This is further illustrated in the zoomed fig.13. Proposed technique operated in mode 3 where no V_{oc} is measured so proposed technique definitely increases the power efficiency. Voltage variations of the two techniques during MPP are also shown in fig.14.

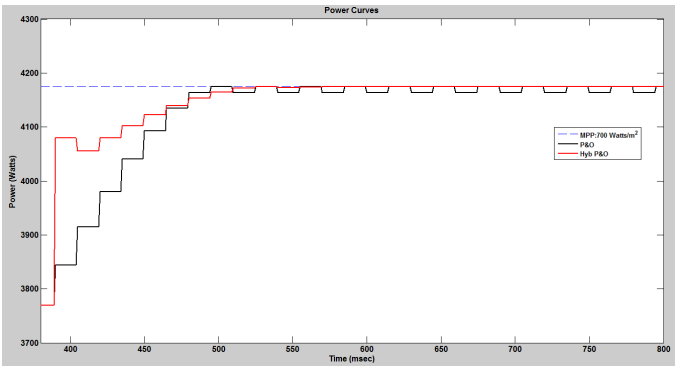

Fig. 12. Performance comparison at fixed irradiance

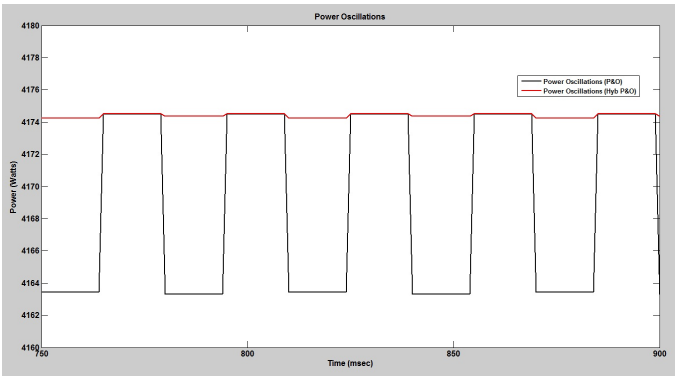

Fig. 13. Comparison of power oscillation around MPP at fixed irradiance

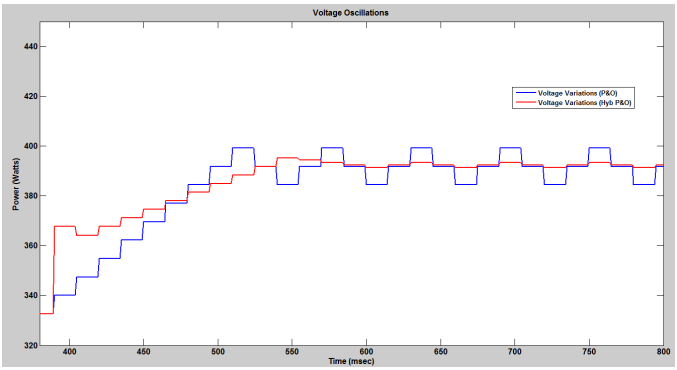

Fig. 14. Comparison of voltage oscillation around MPP at fixed irradiance

B. Dynamic Conditions

1) Under Varying Irradiance: The proposed hybrid method and $P\&O$ are bombarded with severe changing irradiance conditions as shown in fig.15,16 and 17. The lower diagram in each figure indicates the variations in irradiance levels while upper diagram shows the power curves of two techniques. Dotted lines in each upper diagram reveal the maximum power points at different irradiance levels. In all these cases, first both techniques are allowed to settle at irradiance of 700 W/m^2, then they are subjected to different irradiance levels at each sampling time and after that they are again allowed to settle at a particular irradiance. It can be seen from fig.15,16 and 17 that proposed technique focuses MPP more efficiently and effectively than $P\&O$ and even when the irradiance gets settled; it is able to reach MPP almost at the same time even with smaller step size as compared to $P\&O$. Three arrows with blue, red and black are marked in each figure to give users the better understanding of results. Where blue arrow represents the MPP at that time instant while red arrow depicts the proposed technique response and black arrow represents the $P\&O$ response at that instant. It can be seen with the help of arrows that how much the proposed technique is closed to MPP while $P\&O$ struggles to get there thus proving the robustness of the proposed technique

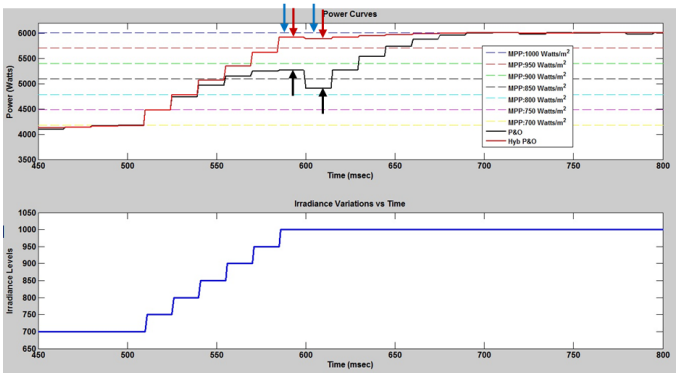

Fig. 15. Testing of proposed and P&O techniques under increasing irradiance

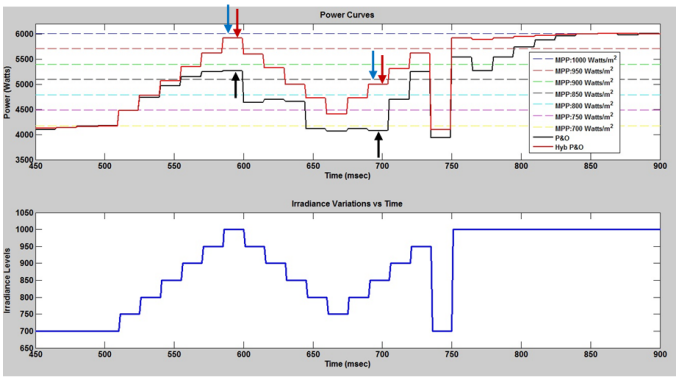

Fig. 16. Testing of proposed and P&O techniques under varying irradiance

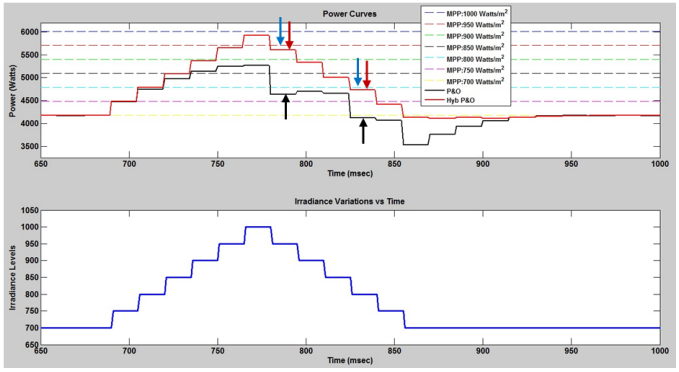

Fig. 17. Testing of proposed and P&O techniques under varying irradiance

2) Under varying temperature: Figure 18 shows the performance of proposed scheme and conventional $P\&O$ method under varying temperature. The temperature is varied with a step size of 0.5 C° and it can be seen that proposed technique is following the changes more swiftly than the $P\&O$ technique.

V. Conclusion

In this paper we have proposed a new technique for tracking the maximum power point. Our technique is a hybrid of two well known techniques for MPPT but is equipped with intelligent thinking and therefore has following advantages

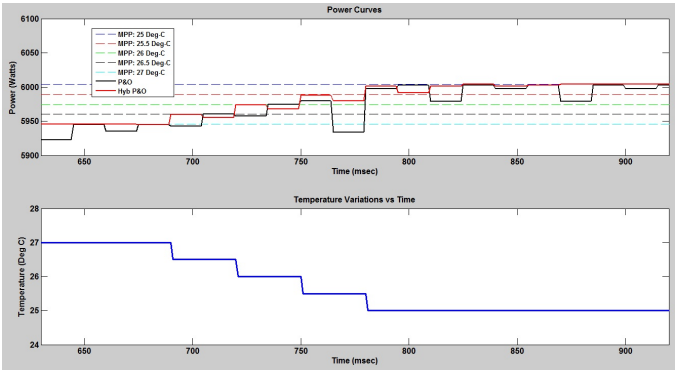

Fig. 18. Testing of proposed and P&O techniques under varying temperature

over the conventional techniques.

- In mode 1, try to skip region 1. Advantage:Reach MPP region quickly.
- In mode 2, comparison is being made with 0.76 V_{oc}. Advantage: In case of moving away from MPP as often is the case in $P\&O$ during environmental variations, this will put us write back in the region of MPP.
- In mode 3, limits are checked i.e. PLL $\leq P \leq$ PUL . Advantage: Don't have to check V_{oc} during this period so power will not be interrupted to load. As step size is reduced so drastically therefore oscillation around the maximum power will be less.

References

[1] T. Esram and P. Chapman, "Comparison of photovoltaic array maximum power point tracking techniques," *Energy conversion, IEEE transactions on*, vol. 22, no. 2, pp. 439–449, 2007.

[2] M. Moradi and A. Reisi, "A hybrid maximum power point tracking method for photovoltaic systems," *Solar Energy*, 2011.

[3] G. Yu, Y. Jung, J. Choi, and G. Kim, "A novel two-mode mppt control algorithm based on comparative study of existing algorithms," *Solar Energy*, vol. 76, no. 4, pp. 455–463, 2004.

[4] J. Enslin, M. Wolf, D. Snyman, and W. Swiegers, "Integrated photovoltaic maximum power point tracking converter," *Industrial Electronics, IEEE Transactions on*, vol. 44, no. 6, pp. 769–773, 1997.

[5] J. Jiang, T. Huang, Y. Hsiao, and C. Chen, "Maximum power tracking for photovoltaic power systems," *Tamkang Journal of Science and Engineering*, vol. 8, no. 2, p. 147, 2005.

[6] S. Jain and V. Agarwal, "A new algorithm for rapid tracking of approximate maximum power point in photovoltaic systems," *Power Electronics Letters, IEEE*, vol. 2, no. 1, pp. 16–19, 2004.

[7] T. Tafticht and K. Agbossou, "Development of a mppt method for photovoltaic systems," in *Electrical and Computer Engineering, 2004. Canadian Conference on*, vol. 2. IEEE, 2004, pp. 1123–1126.

[8] N. Femia, G. Petrone, G. Spagnuolo, and M. Vitelli, "Optimization of perturb and observe maximum power point tracking method," *Power Electronics, IEEE Transactions on*, vol. 20, no. 4, pp. 963–973, 2005.

[9] M. Villalva, J. Gazoli *et al.*, "Comprehensive approach to modeling and simulation of photovoltaic arrays," *Power Electronics, IEEE Transactions on*, vol. 24, no. 5, pp. 1198–1208, 2009.

[10] H. Tsai, C. Tu, and Y. Su, "Development of generalized photovoltaic model using matlab/simulink," in *Proceedings of the World Congress on Engineering and Computer Science*. Citeseer, 2008, pp. 846–851.

[11] C. Carrero, J. Amador, and S. Arnaltes, "A single procedure for helping pv designers to select silicon pv modules and evaluate the loss resistances," *Renewable Energy*, vol. 32, no. 15, pp. 2579–2589, 2007.

[12] M. Villalva, J. Gazoli *et al.*, "Modeling and circuit-based simulation of photovoltaic arrays," in *Power Electronics Conference, 2009. COBEP'09. Brazilian.* Ieee, 2009, pp. 1244–1254.